# 8 Appendix

## 8.1 Appendix A

### Comparison of dual permeability model with standard model

The dual permeability model with all five hydraulic conductivity variants were compared to the standard model by setting the fracture and matrix domain the same with parameterization in Tab. 20. Fig. 25 shows the results of the scenarios. The dual permeability models outputs are identical to the standard output. Simulation output in Fig. 25 make it hard to identify any gray lines indicating the dual permeability model as the alignment with the standard model is too good. The exchange boundary conductivity $K_a$ is non-zero for scenario 1, 2 and 3. Fig. 26 shows a ponding scenario with free drainage (scenario 4) at the bottom for the set up as in Tab. 20. The output times reflect the beginning of the simulation, where deviations between the standard model and the dual permeability model are noticeable. The modified set-up included a decreased Picard iteration criterion, decreased maximum time-step and direct evaluation of the constitutive equations. The modified set-up improved the simulation. In both set-ups the dual permeability model converges towards the standard model.

Table 20: Soil hydraulic properties and domain description used in test simulations of the dual permeability model with the standard model.

| **Parameter** | **Symbol** | **Value** |
|---|---|---|
| Inverse of air entry value [$cm^{-1}$] | $\alpha$ | 0.05 |
| Shape parameter | $n$ | 2 |
| Sat. water content [-] | $\theta_s$ | 0.45 |
| Residual water content [-] | $\theta_r$ | 0 |
| Sat. hydraulic conductivity [cm $d^{-1}$] | $K_s$ | 200 |
| Domain length [cm] | $L$ | 10 |
| Spatial discretization [cm] | $dx$ | 0.1 |
| Simulation time [days] | $t$ | 2 |
| Minimum time step [days] | $dt_{min}$ | 5e-8 |
| Maximum time step [days] | $dt_{max}$ | 0.1 |

Table 21: Initial and boundary conditions used for test simulations of the dual permeability model with the standard model in *DRUtES*.

| **Scenario** | **Initial $h_{pres}$** | **Top bc** | **Bottom bc** |
|---|---|---|---|
| 1 | -100 cm | -50 cm | -50 cm |
| 2 | -100 cm | 0.5 cm $d^{-1}$ | -100 cm |
| 3 | -10 cm | -0.2 cm $d^{-1}$ | -10 cm |
| 4 | -50 cm | 0 cm | free drainage |

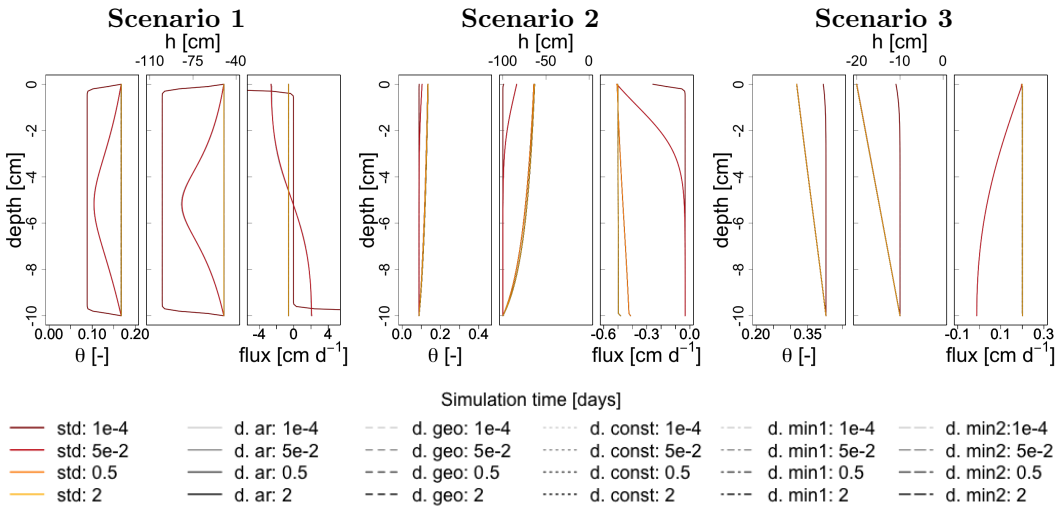


Figure 25: Simulation output after 1e-4, 5e-2, 0.5 and 2 days of test scenarios 1, 2 and 3. The gray lines cannot be recognized because the dual variants and the standard model align perfectly.

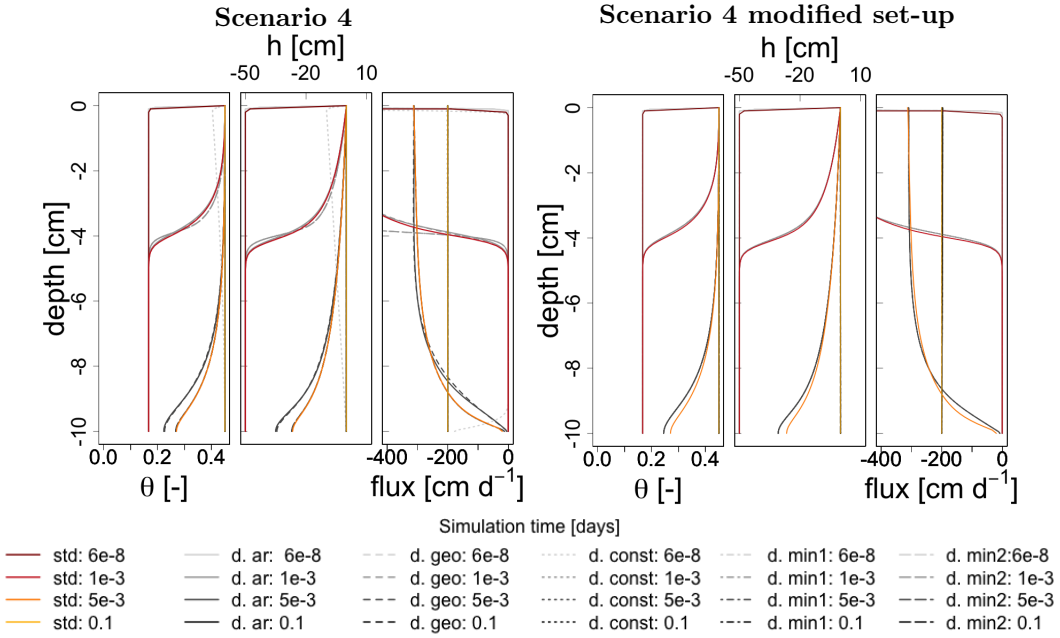


Figure 26: Simulation output after 6e-8, 1e-3, 5e-3 and 0.1 days of test scenarios 4 with different set-up

## 8.2 Appendix B

Fig. 27 depicts boxplots of 30D CEC Benchmark functions without any reinitialization during the optimization. Comparing these to calibrated optimization output, it becomes evident that, generally, reinitialization can enhance the optimization result immensely in most cases.

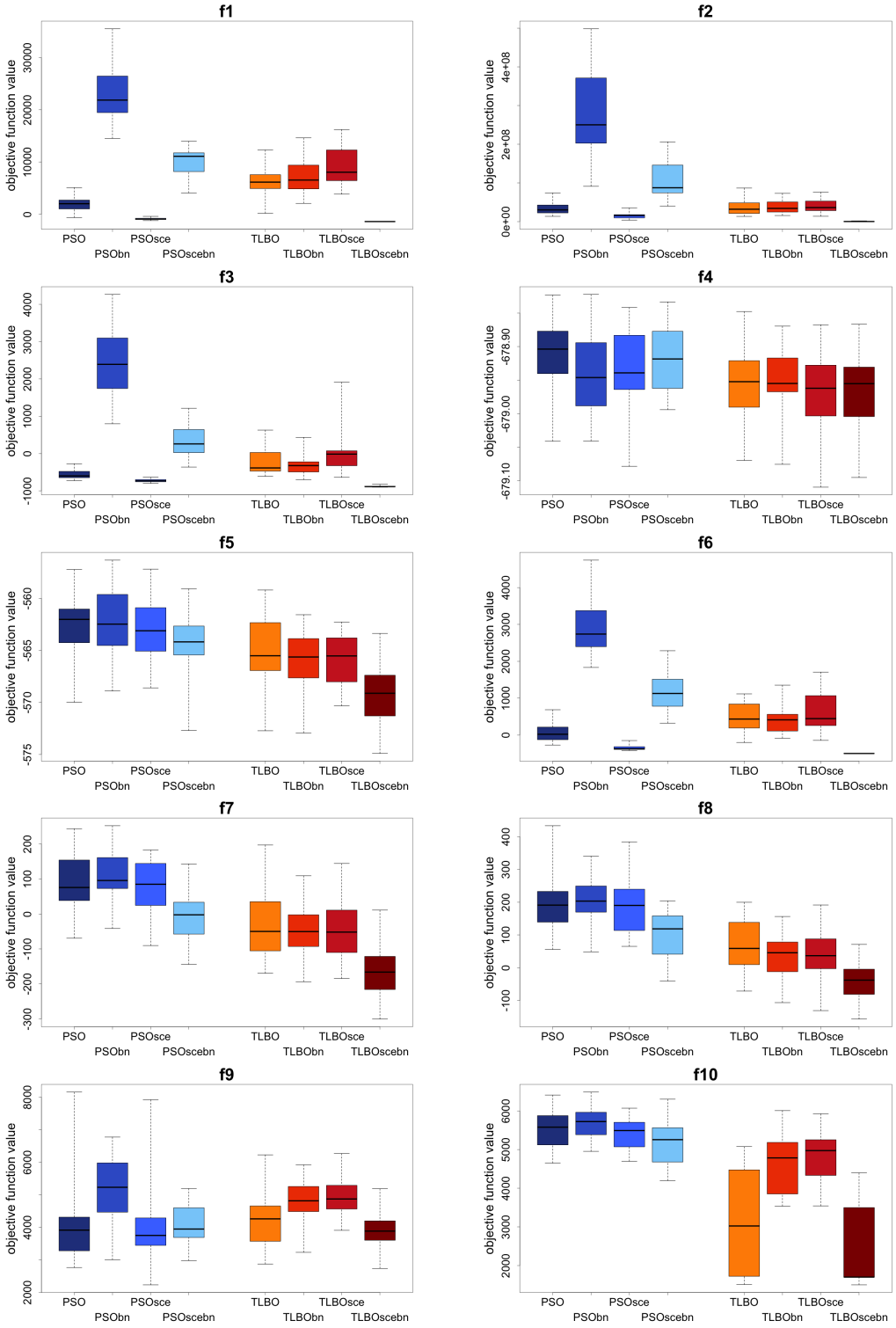


Figure 27: Boxplots of 30 runs of 30D benchmark functions without reinitialization.